Magnetic exchange in α-iron from *ab initio* calculations in the paramagnetic phase

P. A. Igoshev,[1,2] A. V. Efremov,[1] and A. A. Katanin[1,2]

[1]*Institute of Metal Physics, Russian Academy of Sciences, 620990 Ekaterinburg, Russia*
[2]*Ural Federal University, 620002 Ekaterinburg, Russia*

Applying the local density approximation (LDA) and dynamical mean field theory to paramagnetic α-iron, we reinvestigate the origin of its ferromagnetism. The analysis of local magnetic susceptibility shows that at sufficiently low temperatures $T < 1500$ K, both e_g and t_{2g} states equally contribute to the formation of the effective magnetic moment with spin $S = 1$. The self-energy of t_{2g} states shows sizable deviations from Fermi-liquid form, which accompany earlier found nonquasiparticle form of e_g states. By considering the nonuniform magnetic susceptibility we find that the nonquasiparticle form of e_g states is crucial for ferromagnetic instability in α-iron. The main contribution to the exchange interaction, renormalized by the effects of electron interaction, comes from the hybridization between t_{2g} and e_g states. We furthermore suggest the effective spin-fermion model for α-iron, which allows us to estimate the exchange interaction from paramagnetic phase, which is in agreement with previous calculations in the ordered state within the LDA approaches.

Elemental iron in its low-temperature body-centered cubic (bcc) phase, which is stable below approximately 1200 K, provides a unique example of itinerant magnetic d-electron systems, where formation of well-defined local magnetic moments can be expected. Indeed, the Rhodes-Wolfarth ratio p_C/p_S for this substance is very close to one, which is a characteristic feature of systems, containing (almost) localized d electrons [p_C corresponds to the magnetic moment, extracted from the Curie-Weiss law for magnetic susceptibility in the paramagnetic phase $\chi = (g\mu_B)^2 p_C(p_C + 1)/(3T)$, and p_S is the saturation moment (in units of $g\mu_B$), g is a Landé factor, and T denotes temperature]. At the same time, the moment $p_C = 1.1$ has a small fractional part, which is natural for the itinerant material.

This poses the following natural questions. Which electrons mainly contribute to the local-moment spin degrees of freedom of α-iron? What is the appropriate physical model, that describes spin degrees of this substance? Attempting to answer the former question, Goodenough suggested [1] that the e_g electrons are localized, while t_{2g} electrons are itinerant. This suggestion was later on refined in Ref. [2], pointing to a possibility that only some fraction of e_g electrons, contributing to formation of the peak of the density of states near the Fermi level, named by the authors as a giant van Hove singularity, is localized. (The intimate relation between peaks of density of states and electron localization was also previously pointed out in Ref. [3]). On the contrary, there were statements made that 95% of electrons are localized in iron [4]. On the model side, the thermodynamic properties of α-iron were described within the effective spin $S = 1$ Heisenberg model [5], assuming therefore that the main part of the magnetic moment is localized, in agreement with the above-mentioned Rhodes-Wolfarth arguments. Use of the effective Heisenberg model was justified from the *ab initio* analysis of spin spiral energies yielding reasonable values of the exchange integrals [6].

These considerations however did not take into account strong electronic correlations in α-iron, the important role of which was emphasized first in Ref. [7]. Previous calculations [8,9] within the local density approximation (LDA), combined with the dynamical mean-field theory (DMFT), revealed the presence of nonquasiparticle states formed by e_g electrons, which were considered as a main source of local moment formation in iron, while t_{2g} states were assumed to be itinerant [8]. At the same time, magnetic properties of the same t_{2g} states also show some features of local-moment behavior. In particular, the temperature dependence of inverse local spin susceptibility, which was calculated previously [8] only at $T > 1000$ K because of the limitations of the Hirsch-Fye method, is approximately linear, including the contribution of t_{2g} states; the real part of t_{2g} contribution to dynamic local magnetic susceptibility has a peak at low frequencies, reflecting a possibility of partial local moment formation by t_{2g} states.

Studying this possibility requires investigation of electronic and magnetic properties at low temperatures, since the energy scale for partially formed local t_{2g} moments can be smaller than for e_g states. Although real substance orders ferromagnetically at low temperatures, in the present paper (as in Ref. [8]) we perform analysis of local properties of iron in the paramagnetic phase to reveal the mechanism of local moment formation. Furthermore, we study nonlocal magnetic susceptibility in the low temperature range $T > 250$ K, which allows us to analyze the mechanism of magnetic exchange. To this end we use the state-of-art dynamical mean-field theory (DMFT) calculation with a continous time quantum Monte Carlo (CT-QMC) solver [10], combined with the *ab initio* local density approximation (LDA). From our low-temperature analysis, we argue that t_{2g} electrons almost equally contribute to the effective local magnetic moment, as the e_g electrons, and play a crucial role in the mechanism of magnetic exchange in iron. In particular, the most important contribution to the exchange integrals comes from the hybridization of t_{2g} and e_g states, which yields *nearest-neighbor* magnetic exchange interaction, which agrees well with the experimental data.

We perform the *ab initio* band-structure calculations in LDA approximation within tight-binding–linear muffin-tin orbital–atomic spheres approximation framework, the von Barth–Hedin local exchange-correlation potential [11] was
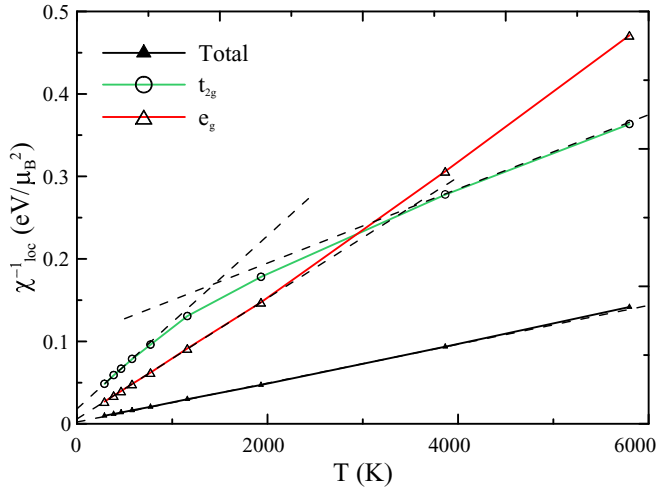
FIG. 1. (Color online) Temperature dependence of inverse local magnetic susceptibility, and the corresponding e_g and t_{2g} orbital contributions. Dashed lines show linear behavior in different temperature intervals.

used. Primitive reciprocal translation vectors were discretized into 12 points along each direction which leads to 72 **k** points in the irreducible part of the Brillouin zone. For DMFT (CT-QMC) calculations, we use the Hamiltonian of Hubbard type with the kinetic term containing all s-p-d states, being extracted from the LDA solution, and the interaction part with density-density contributions for d electrons only. The Coulomb interaction parameter value $U = 2.3$ eV and the Hund's parameter $I = 0.9$ eV used in our work are the same as in earlier LDA+DMFT calculations [7,8,13]. To treat a problem of formation of local moments we consider a paramagnetic phase, which is achieved by assuming spin-independent density of states, local self-energy, and bath Green function. For the purpose of extracting corresponding exchange parameters, we take in LDA part physical value of the lattice parameter $a = 2.8664$ Å, corresponding to the ferromagnetic state at room temperature.

We consider first the results for the orbital-resolved temperature-dependent local static spin susceptibility $\chi_{\mathrm{loc},mn} = 4\mu_B^2 \int_0^\beta \langle s_{i,m}^z(\tau) s_{i,n}^z(0)\rangle d\tau$, where $s_{i,m}^z$ is the z projection of the spin of d electrons, belonging to the orbitals $m = t_{2g}, e_g$ at a given lattice site i; see Fig. 1 (for completeness, we also show the total susceptibility $\chi_{\mathrm{loc}} = \sum_{mn} \chi_{\mathrm{loc},mn}$, which also includes the off-diagonal t_{2g}-e_g contribution). The temperature dependence of the static inverse local susceptibility is linear (as was also observed in previous studies [7–9,13]); however being resolved with respect to orbital contributions (see Fig. 1) it appears to manifest a very different nature of e_g and t_{2g} moments. The inverse e_g orbital contribution behaves approximately linearly with T in a broad temperature range [8,9]. At the same time, analyzing low-temperature behavior, we find that $\chi_{\mathrm{loc},t_{2g}\text{-}t_{2g}}^{-1}$ demonstrates a crossover at $T^* \sim 1500$ K between two linear dependences with the low-temperature part having higher slope (i.e., smaller effective moment). Note that this feature was not obtained in a previous study [8] because of considering only temperature range $T > 1000$ K. The scale T^* corresponds to the crossover to non-Fermi-liquid behavior of t_{2g} states; see below.
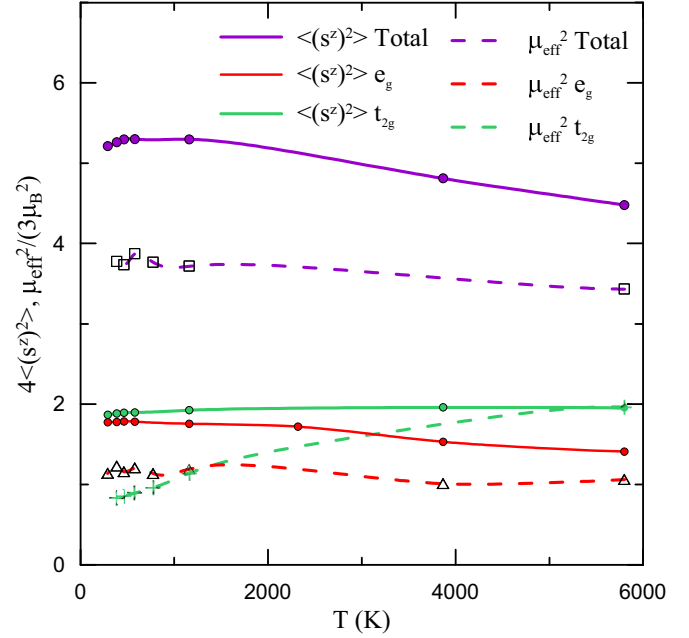

FIG. 2. (Color online) Temperature dependence of the effective magnetic moment and instantaneous average $\langle (s^z)^2\rangle$ and μ_{eff}^2 in α-iron, extracted from the temperature dependence of local susceptibility, together with the contribution of the e_g and t_{2g} orbitals.

To get further insight into the local magnetic properties of α-iron, we consider the temperature dependence of the effective magnetic moment $\mu_{m,\mathrm{eff}}^2 = 3/(d\chi_{\mathrm{loc},mm}^{-1}/dT)$ and the instantaneous average $\langle (s_{i,m}^z)^2\rangle$, corresponding to different orbital states; see Fig. 2. We find that for e_g electrons both moments saturate at temperatures $T < 1500$ K and remain approximately constant up to sufficiently low temperatures. Comparing the value of the square of the moment $\mu_{e_g,\mathrm{eff}}^2/(3\mu_B^2) = 1.2$, extracted from the Curie-Weiss law for local susceptibility, and the instantaneous average $4\langle (s_{i,e_g}^z)^2\rangle = 1.8$ with the corresponding filling $n_{e_g} \simeq 2.6$, we find that the major part of e_g electrons determine the instantaneous average $\langle (s_{i,e_g}^z)^2\rangle$, and at least half of them contribute to the sufficiently long-living (on the scale of $1/T$) local moments. At the same time, for t_{2g} electronic states the abovementioned crossover between the high-temperature value $\mu_{t_{2g},\mathrm{eff}}^2/(3\mu_B^2) \approx 1.95$ and the low temperature value $\mu_{t_{2g},\mathrm{eff}}^2/(3\mu_B^2) \simeq 0.82$ is present, which, comparing to $n_{t_{2g}} \simeq 4.4$, shows that at least 20% of t_{2g} electrons participate in the effective local moment formation at low temperatures. Yet, the corresponding low-temperature effective moments $\mu_{e_g,\mathrm{eff}}^2$ and $\mu_{t_{2g},\mathrm{eff}}^2$ are comparable (each of them is approximately $3\mu_B^2$, corresponding to the effective spin $s \simeq 1/2$), showing the important role of t_{2g} electrons in the formation of the total spin $S = 1$ state.

Although the self-energy calculations [8,9] yield a quasiparticlelike form of t_{2g} electron self-energy, the low-frequency and low-temperature dependence of self-energy shows pronounced deviations from the Fermi-liquid behavior; see Fig. 3. To analyze the frequency dependence of the self-energy on the imaginary frequency axis, we fit the obtained results by the Fermi-liquid dependence $-\mathrm{Im}\Sigma(i\nu) = \Gamma(T) + [Z^{-1}(T) - 1]\nu + \sigma(T)\nu^2$, where $\Gamma(T)$ is the damping of
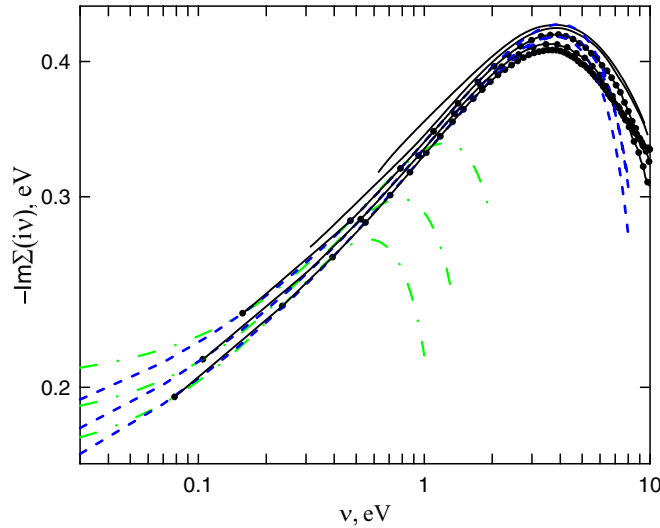
FIG. 3. (Color online) Frequency dependence of $\mathrm{Im}\Sigma_{t_{2g}}(i\nu)$ (black solid lines), calculated at Matsubara frequencies $\nu_n = \pi T(2n+1)$ (marked by dots) at temperatures (from top to bottom) $T = 1/5, 1/10, 1/20, 1/30, 1/40$ eV. The green dot-dashed line presents fits to the Fermi-liquid dependence in the range $\nu_n < 1$ eV, while blue dashed lines present fits to the non-Fermi-liquid dependence (see text).

electrons at the Fermi level and $Z(T)$ is the temperature-dependent quasiparticle residue. Alternatively, we consider the fit $-\mathrm{Im}\Sigma(i\nu) = \Gamma_1(T) + \beta_1(T)\nu^\alpha + \sigma_1(T)\nu^2$ with some exponent $\alpha < 1$. The latter dependence corresponds to the non-Fermi-liquid behavior of t_{2g} electrons. The obtained results are presented in Table I.

The linear-quadratic fits are applicable only at $\nu < 1$ eV; at sufficiently small ν they also do not fit the obtained results well. We find that the spectral weight $Z(T)$ pronouncely decreases with decrease of temperature, and the coefficient $\Gamma(T)$ obviously does not obey the Fermi-liquid dependence $\Gamma(T) \propto T^2$. These observations show that sizable deviations from the Fermi-liquid picture can be expected.

The power-law fits yield much better agreement in a broad range of frequencies $\nu < 5$ eV, describing at the same time correctly the low-frequency behavior. The coefficients β_1, σ_1 of these fits show very weak temperature dependence (the contribution σ_1 is almost negligible), while the damping $\Gamma_1(T)$ and the exponent α slightly decrease with temperature, being related by $\Gamma_1(T) \sim T^\alpha$. These observations imply that t_{2g} electronic subsystem is better described by non-Fermi-liquid behavior at low temperatures, which reflects its participation in the formation of local moments in α-iron. Remarkably,

TABLE I. Parameters of the fits of frequency dependence of $\mathrm{Im}\Sigma(i\nu)$ to the Fermi-liquid and non-Fermi-liquid forms at different temperatures.

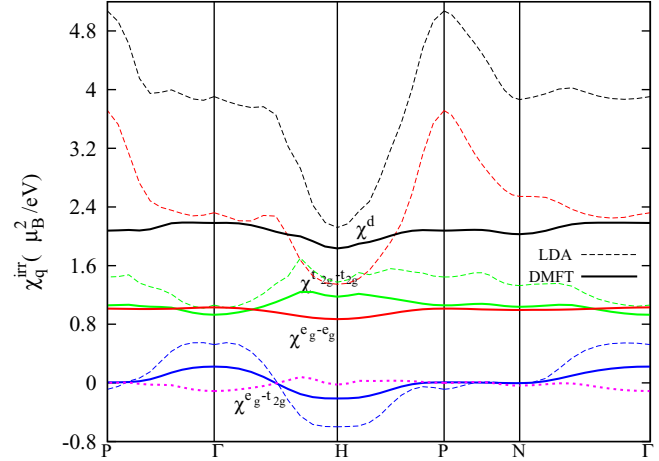| $\beta = 1/T$	Γ	$Z^{-1}-1$	σ	Γ_1	β_1	σ_1	α
20	0.20	0.22	−0.09	0.17	0.18	−0.006	0.51
30	0.18	0.29	−0.19	0.15	0.19	−0.005	0.48
40	0.17	0.37	−0.32	0.13	0.20	−0.005	0.44

FIG. 4. (Color online) Orbital-resolved momentum dependence of $\chi_{\mathbf{q}}^{0,mn}$ at $T = 290$ K calculated in high symmetry directions of the Brillouin zone. The contributions $\chi_{\mathbf{q}}^{0,d}$, $\chi_{\mathbf{q}}^{0,t_{2g}-t_{2g}}$, $\chi_{\mathbf{q}}^{0,e_g-e_g}$, and the hybridization part $\chi_{\mathbf{q}}^{0,e_g-t_{2g}}$ are shown by black, red, green, and blue lines, respectively. Solid (dashed) lines correspond to LDA+DMFT (LDA) results. The LDA+DMFT estimate for $J_q^{(1)}(\mu_B/I)^2$ is shown by magenta short-dashed line.

consideration of the three-band model in Ref. [12] showed similar dependence of the self-energy $\Sigma \sim \nu^{1/2}$ due to Hund exchange interaction, which allows us to attribute the t_{2g} subsystem in iron as close to the "spin freezing" transition, according to the terminology of Ref. [12].

To get further insight into the formation of effective local moments and extract corresponding exchange integrals, we calculate the momentum dependence of particle-hole bubble $\chi_{\mathbf{q}}^{0,mn} = -(2\mu_B^2/\beta)\sum_{l,\mathbf{k},\widetilde{m}\in m,\widetilde{n}\in n}\mathcal{G}_{\mathbf{k},\widetilde{m}\widetilde{n}}(i\nu_l)\mathcal{G}_{\mathbf{k}+\mathbf{q},\widetilde{n}\widetilde{m}}(i\nu_l)$, which is obtained using paramagnetic LDA and LDA+DMFT electronic spectrum [$\mathcal{G}_{\mathbf{k},\widetilde{m}\widetilde{n}}(i\nu_l)$ is the corresponding electronic Green function for the transition from the orbital state $\widetilde{m}$ to $\widetilde{n}$, and ν_l is a fermionic Matsubara frequency; for more details on the calculation procedure see Ref. [13]]. The results for LDA and LDA+DMFT approaches at $T = 290$ K are presented in Fig. 4 (we find that the LDA+DMFT results are almost temperature independent at low T). For the bubble, calculated using purely LDA spectrum (i.e., with the assumption that all electrons are itinerant), the maximum of $\chi_{\mathbf{q}}^0$ is located at the point $\mathbf{q} = \mathbf{q}_P = (\pi, \pi, \pi)/a$, while the ferromagnetic instability in α-iron requires a maximum of $\chi_{\mathbf{q}}^0$ at $\mathbf{q} = 0$ and low T, if one neglects the nonlocal vertex corrections. One can observe that the main contribution to this behavior of the bubble originates from the e_g electron part, $\chi_{\mathbf{q}}^{0,e_g-e_g}$. Both $\chi_{\mathbf{q}}^{0,e_g-e_g}$ and $\chi_{\mathbf{q}}^{0,e_g-t_{2g}}$ contributions are however strongly influenced by the account of the local self-energy corrections to the Green's function in the DMFT approach, which correspond physically to the account of partial localization of d electrons. These corrections mainly change $\chi_{\mathbf{q}}^{0,e_g-e_g}$ and shift the maximum of $\chi_{\mathbf{q}}^0$ to Γ point ($\mathbf{q} = 0$). Note that within LDA+DMFT, intraorbital contributions to $\chi_{\mathbf{q}}^{0,e_g-e_g}$ and $\chi_{\mathbf{q}}^{0,t_{2g}-t_{2g}}$ are only weakly momentum dependent; they also behave similarly, varying "counterphase." According to the general ideas of spin-fluctuation theory [14], this weak momentum

dependence can be ascribed to the formation of the effective moments from e_g and t_{2g} states. In agreement with the above discussed consideration, the $\chi_{\mathbf{q}}^{0,e_g-e_g}$ contribution has even weaker dispersion than the $\chi_{\mathbf{q}}^{0,t_{2g}-t_{2g}}$ part. At the same time, strongly dispersive $\chi_{\mathbf{q}}^{0,e_g-t_{2g}}$ contribution, which is assumed to correspond to the (remaining) itinerant degrees of freedom, provides the maximum of the resulting $\chi_{\mathbf{q}}^0$ at $\mathbf{q} = 0$ and appears to be the main source of the stability of the ferromagnetic ordering in iron within LDA+DMFT approximation. The obtained results do not change qualitatively for the other choice Hubbard interactions (as we have verified for $U = 4.0$ and $I = 1.0$ eV); see Appendix A.

To see the quantitative implications of the described physical picture, we consider the effective spin-fermion model

$$
\begin{aligned}
\mathcal{S} = \frac{1}{2} \sum_{i,j,\mathbf{q},\omega_n} & \chi_S^{-1}(\mathbf{q},i\omega_n) \mathbf{S}_i(i\omega_n) \mathbf{S}_j(-i\omega_n) e^{i\mathbf{q}(\mathbf{R}_i - \mathbf{R}_j)} \\
& + 2I \sum_{i,\omega_n} \mathbf{S}_i(i\omega_n) \mathbf{s}_i(-i\omega_n) \\
& + \sum_{\nu_n \sigma l l'} c_{l\sigma}^{\dagger}(i\nu_n) \left[-i\nu_n \delta_{ll'} + H_{ll'} + \Sigma_{ll'}(i\nu_n) \right] c_{l'\sigma}(i\nu_n)
\end{aligned}
\tag{1}
$$

(ω_n is a bosonic Matsubara frequency; l,l' combines site and orbital indices), describing interaction of itinerant electrons with (almost) *local* spin fluctuations (in contrast to critical spin fluctuation in cuprates [15]); see also Ref. [16]. We assume here that the Coulomb and Hund's interaction acting within e_g and t_{2g} orbitals results in a formation of some common local moment (field $\mathbf{S}$), while the remaining itinerant degrees of freedom are described by the field $\mathbf{s}_i = \mathbf{s}_i^{e_g} + \mathbf{s}_i^{t_{2g}}$, formed from the Grassmann variables $c_{l'\sigma}$; $H_{ll'}$ and $\Sigma_{ll'}$ are the Hamiltonian and local self-energy corrections to the LDA spectrum (the latter is assumed to be local and therefore diagonal with respect to orbital indices). The interaction between the two subsystems (localized and itinerant), which are formed from the d-electronic states, is driven by Hund's constant coupling I.

Considering the renormalization of the propagator χ_S by the corresponding boson self-energy corrections, we obtain for the nonuniform susceptibility (see Appendix B)

$$
\chi^{-1}(\mathbf{q},i\omega_n) = \chi_{\mathrm{loc}}^{-1}(i\omega_n) - J_{\mathbf{q}} / (4\mu_B^2),
\tag{2}
$$

where $\chi_{\mathrm{loc}}(i\omega_n)$ is the local spin susceptibility and $J_{\mathbf{q}}$ is the exchange interaction, which fulfills $\sum_{\mathbf{q}} J_{\mathbf{q}} = 0$ (no spin self-interaction). We find $J_{\mathbf{q}} = J_{\mathbf{q}}^{(1)} + J_{\mathbf{q}}^{(2)}$, $J_{\mathbf{q}}^{(1)} = (I/\mu_B)^2 \sum_m [\chi_{\mathbf{q}}^{0,mm} - \sum_{\mathbf{p}} \chi_{\mathbf{p}}^{0,mm}]$ is the intraorbital part, while $J_{\mathbf{q}}^{(2)} = 2(I/\mu_B)^2 \chi_{\mathbf{q}}^{0,t_{2g}-e_g}$ results from the hybridization of states of different symmetry. The contribution $J_{\mathbf{q}}^{(1)}$ is approximately twice smaller than $J_{\mathbf{q}}^{(2)}$, and therefore the main contribution to the magnetic exchange comes from the hybridization of t_{2g} and e_g states. The whole momentum dependence of $J_{\mathbf{q}}^{(2)}$ can be well captured by the nearest-neighbor approximation for effective exchange integrals only, $J_{\mathbf{q}}^{(2)} = J_0 \cos(aq_x/2) \cos(aq_y/2) \cos(aq_z/2)$, while $J_{\mathbf{q}}^{(1)}$ has more complicated momentum dependence.

Restricting ourselves by considering the contribution $J_{\mathbf{q}} = J_{\mathbf{q}}^{(2)}$ (we assume that the contribution $J_{\mathbf{q}}^{(1)}$ is further suppressed by the nonlocal and vertex corrections), from Fig. 1 we find at $T = 290$ K the value $J_{\mathbf{q}=0} = 0.18$ eV. This value, as well as the momentum dependence of $J_{\mathbf{q}}^{(2)}$, agrees well with the result of Okatov *et al.* [6]. The obtained results together with $\mu_{\mathrm{eff}}^2 = 11.4\mu_B^2$ (see Fig. 2) provide an estimate for the Curie temperature, which can be obtained from the divergence of $\chi^{-1}(\mathbf{q},0)$:

$$
T_C = \frac{\mu_{\mathrm{eff}}^2}{4\mu_B^2} \frac{J_0}{3} = 0.17 \text{ eV},
\tag{3}
$$

and appears comparable with the result of full DMFT calculation, and therefore shows that the above model is adequate for describing magnetic properties of the full five-band Hubbard model. [Note that the overestimation of T_C in DMFT approach in comparison with the experimental data is due to density-density approximation for the Coulomb interaction [17] and due to the presence of nonlocal fluctuations, not accounted for by DMFT.]

Neglecting longitudinal fluctuations of field $\mathbf{S}$ we can map the model (1) to an effective $S = 1$ Heisenberg model $\mathcal{H}_{\mathrm{H}} = (1/2) \sum_{ij} J_{ij} \mathbf{S}_i \mathbf{S}_j$ to estimate the spin-wave spectrum:

$$
\omega_{\mathbf{q}} = S(J_0 - J_{\mathbf{q}}) = S(I/\mu_B)^2 \left(\chi_0^{0,e_g-t_{2g}} - \chi_{\mathbf{q}}^{0,e_g-t_{2g}} \right).
\tag{4}
$$

We obtain the corresponding spin stiffness $D = \lim_{q \to 0}(\omega_{\mathbf{q}}/q^2) = 290$ meV Å^2 in a good agreement with the experimental data $D = 280$ meV Å^2 (Ref. [18]).

In conclusion, we have considered the problem of the description of effective local moments in α-iron based on the electronic spectrum in a paramagnetic phase within the LDA+DMFT approximation. We find that local moments are formed by both e_g and t_{2g} orbital states, each of them contributing a half of the total moment $S = 1$. For t_{2g} electronic states we find pronounced features of non-Fermi-liquid behavior, which accompanies an earlier observed nonquasiparticle form of e_g states. The local moment and itinerant states interact with itinerant states via Hund interaction, yielding magnetic exchange between the local-moment states via the effective RKKY-type mechanism. The obtained exchange integrals are well captured by the LDA+DMFT approach. The main origin of the intersite interaction of these moments is attributed to the e_g-t_{2g} hybridization, which yields magnetic exchange, dominating on the nearest-neighbor sites. Contrary to the previous studies [6,19], we do not however assume some magnetic ordering for the electronic system.

We also emphasize that nonlocal self-energy corrections, as well as vertex corrections, missed in our investigation, can make the described physical picture more precise. In particular, nonlocal effects allow for the nonzero nondiagonal e_g-t_{2g} self-energy matrix elements and therefore possibly renormalize the strength of exchange interaction, as well as the self-energy of t_{2g} electronic states. The role of the vertex corrections, only roughly accounted for in the considered approach, also requires additional study. Therefore, further investigation using powerful theoretical techniques of dynamic vertex approximation [20], dual fermion [21], or other nonlocal approaches is of certain interest.

APPENDIX A: LOCAL AND NONUNIFORM SUSCEPTIBILITIES FOR $U = 4$ eV

We test below the stability of our results to change of model parameter values: results of the calculations by using the same method as in the main text but the other choice of parameters ($U = 4.0$ and $I = 1.0$ eV), which are close to those of Ref. [22]. The results for the temperature dependence of the inverse local magnetic susceptibility are shown in Fig. 5. We find the crossover discussed in the main text at lower $T^* \sim 1050$ K. The calculation of momentum dependent irreducible susceptibility yields only the uniform (with respect to **q**) renormalization without change of qualitative tendencies (see Fig. 6; cf. Fig. 4 of the main text). We have recalculated exchange interactions from these results and obtain $J_{\mathbf{q}=0}^{(2)} = 0.13$ eV vs 0.18 eV in the main text. This implies lowering of the Curie temperature, which agrees with approximate renormalization of T^* by 1.5 times (cf. Fig. 1 of the main text). The qualitative conclusions of the paper remain unchanged for these parameter values.

APPENDIX B: CALCULATION OF EXCHANGE INTERACTION FROM THE SPIN-FERMION MODEL

To obtain exchange interaction, we first determine the bare propagator of magnetic degrees of freedom $\chi_S(\mathbf{q}, i\omega_n)$ by requiring that the dressed propagator of **S** field is equal to the susceptibility of the itinerant subsystem. Using the random-phase-type approximation, which reduces the orbital
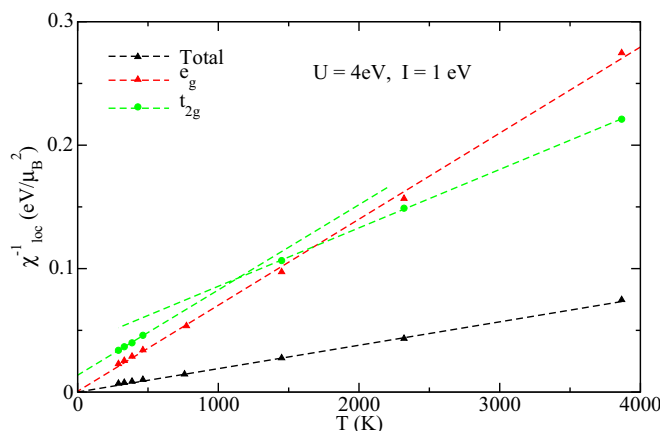

FIG. 5. (Color online) The same as in Fig. 1 of the main text for $U = 4.0$ and $I = 1.0$ eV.
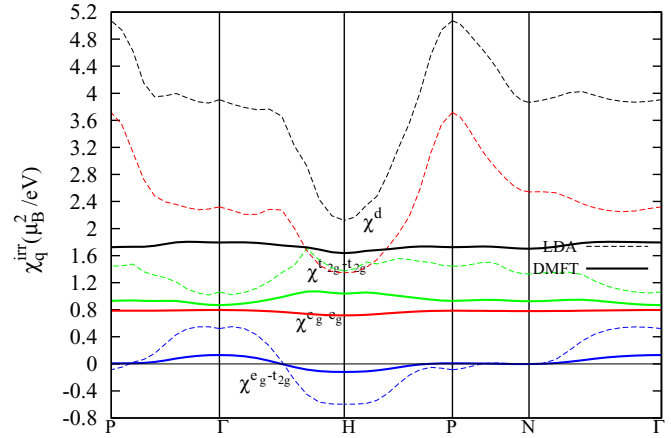

FIG. 6. (Color online) The same as in Fig. 4 of the main text for $U = 4.0$ and $I = 1.0$ eV.

and frequency dependence of the bubble and vertex to the respective frequency and orbital "averaged" quantities, $\chi_q^0 = \sum_{mn} \chi_q^{0,mn}$ (where $q = (\mathbf{q}, i\omega_n)$) and $\Gamma(i\omega_n)$, we obtain

$$\chi_S^{-1}(\mathbf{q}, i\omega_n) = 4\mu_B^2 \left(\chi_q^0\right)^{-1} - 2\Gamma(i\omega_n) + (I/\mu_B)^2 \chi_q^0, \quad (B1)$$

where the last term is added to cancel the corresponding bosonic self-energy correction from itinerant degrees of freedom to avoid double-counting; cf. Ref. [23]. We represent $\chi_q^0 = \overline{\chi}_0(i\omega_n) + \delta\chi_q^0$ with momentum-independent $\overline{\chi}_0(i\omega_n)$; without loss of generality, we can assume $\sum_{\mathbf{q}} \delta\chi_q^0 = 0$, such that $\overline{\chi}_0(i\omega_n) = \sum_{\mathbf{q}} \chi_q^0$. From the results of Fig. 4 of the main text it follows that $\delta\chi_q^0 \ll \overline{\chi}_0(i\omega_n)$. Expanding Eq. (B1) to first order in $\delta\chi_q^0$, we obtain

$$\chi_S^{-1}(\mathbf{q}, i\omega_n) = 4\mu_B^2 \chi_{\text{loc}}^{-1}(i\omega_n) + (I/\mu_B)^2 \overline{\chi}_0(i\omega_n)$$
$$+ \left[(I/\mu_B)^2 - 4\mu_B^2/\overline{\chi}_0^2(i\omega_n)\right]\delta\chi_q^0, \quad (B2)$$

where $\chi_{\text{loc}}^{-1}(i\omega_n) = 1/\overline{\chi}_0(i\omega_n) - 2\Gamma/(4\mu_B^2)$ is the inverse local susceptibility. In practice, the frequency dependence $\chi_{\text{loc}}(i\omega_n) = \mu_{\text{eff}}^2/(3(T + \theta)(1 + |\omega_n|/\delta))$ can be obtained from the dynamic local spin correlation functions, which are characterized by the temperature-independent moment μ_{eff}, its damping $\delta \propto T$, and the corresponding Weiss temperature θ (see Refs. [8,13]), the latter can be neglected at $T \geqslant T_C$. Since $\overline{\chi}_0 \simeq 2\mu_B^2/\text{eV}$ and $I \simeq 1$ eV the momentum dependence is almost canceled, and we obtain the local bare propagator of spin degrees of freedom,

$$\chi_S^{-1}(\mathbf{q}, i\omega_n) \simeq \chi_S^{-1}(i\omega_n) = 4\mu_B^2 \chi_{\text{loc}}^{-1}(i\omega_n) + (I/\mu_B)^2 \overline{\chi}_0(i\omega_n).$$
$$(B3)$$

Considering the renormalization of the propagator χ_S by the corresponding boson self-energy corrections (cf. Ref. [23]), we obtain for the nonuniform susceptibility

$$\chi^{-1}(\mathbf{q}, i\omega_n) = \frac{1}{4\mu_B^2} \left[\chi_S^{-1}(\mathbf{q}, i\omega_n) - \frac{I^2}{\mu_B^2} \sum_{mn} \chi_q^{0,mn} \right], \quad (B4)$$

which yields Eq. (2) of the main text (we use also here that by symmetry $\sum_{\mathbf{p}} \chi_p^{0,t_{2g}-e_g} = 0$).

[1] J. B. Goodenough, Phys. Rev. **120**, 67 (1960).

[2] V. Yu. Irkhin, M. I. Katsnelson, and A. V. Trefilov, J. Phys.: Condens. Matter **5**, 8763 (1993).

[3] S. V. Vonsovskii, M. I. Katsnelson, and A. V. Trefilov, Fiz. Met. Metalloved. **76**(3), 3 (1993); **76**(4), 3 (1993).

[4] M. B. Stearns, Phys. Rev. B **8**, 4383 (1973); R. Mota and M. D. Coutinho-Filho, *ibid.* **33**, 7724 (1986).

[5] F. Körmann, A. Dick, B. Grabowski, B. Hallstedt, T. Hickel, and J. Neugebauer, Phys. Rev. B **78**, 033102 (2008).

[6] S. V. Okatov, Yu. N. Gornostyrev, A. I. Lichtenstein, and M. I. Katsnelson, Phys. Rev. B **84**, 214422 (2011).

[7] A. I. Lichtenstein, M. I. Katsnelson, and G. Kotliar, Phys. Rev. Lett. **87**, 067205 (2001).

[8] A. A. Katanin, A. I. Poteryaev, A. V. Efremov, A. O. Shorikov, S. L. Skornyakov, M. A. Korotin, and V. I. Anisimov, Phys. Rev. B **81**, 045117 (2010).

[9] L. V. Pourovskii, T. Miyake, S. I. Simak, A. V. Ruban, L. Dubrovinsky, and I. A. Abrikosov, Phys. Rev. B **87**, 115130 (2013).

[10] P. Werner, A. Comanac, L. de'Medici, M. Troyer, and A. J. Millis, Phys. Rev. Lett. **97**, 076405 (2006).

[11] U. von Barth and L. Hedin, J. Phys. C **5**, 1629 (1972).

[12] P. Werner, E. Gull, M. Troyer, and A. J. Millis, Phys. Rev. Lett. **101**, 166405 (2008).

[13] P. A. Igoshev, A. V. Efremov, A. I. Poteryaev, A. A. Katanin, and V. I. Anisimov, Phys. Rev. B **88**, 155120 (2013).

[14] T. Moriya, *Spin Fluctuations in Itinerant Magnets* (Springer-Verlag, Berlin, Heidelberg, 1985).

[15] J. Schmalian, D. Pines, and B. Stojković, Phys. Rev. B **60**, 667 (1999); A. Abanov, A. V. Chubukov, and J. Schmalian, Adv. Phys. **52**, 119 (2003).

[16] A. A. Katanin, A. Toschi, and K. Held, Phys. Rev. B **80**, 075104 (2009).

[17] V. I. Anisimov, A. S. Belozerov, A. I. Poteryaev, and I. Leonov, Phys. Rev. B **86**, 035152 (2012).

[18] H. A. Mook and R. M. Nicklow, Phys. Rev. B **7**, 336 (1973).

[19] A. I. Liechtenstein, M. I. Katsnelson, V. P. Antropov, and V. A. Gubanov, J. Magn. Magn. Mater. **67**, 65 (1987).

[20] See, e.g., A. Toschi, A. A. Katanin, and K. Held, Phys. Rev. B **75**, 045118 (2007); A. Toschi, G. Rohringer, A. A. Katanin, and K. Held, Ann. Phys. (Leipzig) **523**, 698 (2011).

[21] See, e.g., A. N. Rubtsov, M. I. Katsnelson, A. I. Lichtenstein, and A. Georges, Phys. Rev. B **79**, 045133 (2009).

[22] L. V. Pourovskii, J. Mravlje, M. Ferrero, O. Parcollet, and I. A. Abrikosov, Phys. Rev. B **90**, 155120 (2014).

[23] P. A. Igoshev, A. A. Katanin, and V. Yu. Irkhin, JETP **105**, 1043 (2007).